Supporting Information

Text S1. Vegetation module implemented by Beudin et al. (2017)

As in the main text, we describe the equations in the two-dimensional form (*x*-*z* plane; zero velocity in *y*-direction) for convenience, while the equations implemented in ROM are three-dimensional; see Beudin et al. (2017) for the complete equations. The vegetation module implemented by Beudin et al. (2017) is for seagrasses/marshes that were represented by the cylinder drag model. They implemented the vegetation impacts not only on flows but also on wave damping. They also included additional functions of leaf bending considering the flexibility of submerged vegetations. Here we only describe the equations for impacts of rigid vegetation (no bending) on flow; these equations were used for comparison with the newly implemented drag and turbulence model for *Rhizophora* mangrove forests.

The drag by vegetation is calculated using the quadratic drag law as

$$F_{veg}(z) = \frac{1}{2} C_D n_v b_v u(z)^2 \quad \text{(S1)}$$

where F_{veg} is the spatially-averaged vegetation drag (m s^{-2}), z is the height from bed (m), C_D is the drag coefficient, n_v is the number of plants (stems or leaves) per unit area (m^{-2}), b_v is the stem or leaf width (m), and u is the flow velocity (m s^{-1}).

The production of turbulence kinetic energy (TKE) by vegetation drag is expressed as

$$P_w = F_{veg} u \quad \text{(S2)}$$

where P_w is the production of TKE by vegetation-generated wakes (m^2 s^{-3}). The dissipation rate of wakes is expressed as

$$D_w = c_2 \frac{P_w}{\tau_{eff}} = c_2 \frac{P_w}{min(\tau_{free}, \tau_{veg})} \quad \text{(S3)}$$

where D_w is the wake dissipation rate (m^2 s^{-4}), c_2 (1.92) is the constant of the k–ε model, and τ_{eff} (s) are the effective time-scale of wakes, which takes the minimum of time-scale of free turbulence (τ_{free}) and time-scale regulated by spaces between the nearest-neighbor plants (τ_{veg}). These are described as

$$\tau_{free} = \frac{k}{\varepsilon} \quad \text{(S4a)}$$

$$\tau_{veg} = \left(\frac{L^2}{{c_w}^2 P_w}\right)^{1/3} = \left(\frac{s^2}{{c_w}^2 P_w}\right)^{1/3} \quad \text{(S4b)}$$

where k is the TKE ($m^2\ s^{-2}$), ε is the turbulent dissipation ($m^2\ s^{-3}$), c_w is the model constant, which was set as 0.09 in Beudin et al. (2017), and L (m) is the length-scale of wakes, which was set as the mean spacing of nearest-neighbor plants (s) in Beudin et al. (2017) where s is calculated from the density, width, and thickness of stem/leaf.

Text S2. Minor modifications of k–ε model introduced by Beudin et al. (2017)

In Beudin et al. (2017), the time-scale of wakes (τ_{eff}) was defined by the minimum of τ_{free} and τ_{veg} as described in Eq. (S3) in Text S1. However, we noticed the minimum function used for τ_{eff} yields complicated results. This may be because of the interactive feedback between τ_{free} and τ_{veg}, such that a case of $\tau_{eff} = \tau_{veg}$ in Eq. (S3) at one moment affects τ_{free} at the next moment through the equations for k (Eq. 2) and ε (Eq. 3); these in turn will affect τ_{eff} in Eq. (S3). As a result, the original model by Beudin et al. (2017) predicted TKE significantly smaller than the model predictions using the time-scale set as either of τ_{free} and τ_{veg}, which are difficult to interpret (results not shown). This minimum function for the time-scale of wake turbulence has not been well supported by previous theoretical and experimental works. As such, we avoided the use of the minimum function for τ_{eff} in our analysis.

The use of τ_{free} for τ_{eff} corresponds to the time-scale used such as in López and García (2001), Defina and Bixio (2005), and Baptist et al. (2007). However, King et al. (2012) and Liu et al. (2017) found that the use of τ_{veg} for τ_{eff}, which explicitly specifies the length-scale of wakes (L in Eq. S4b), would produce much better results than the use of τ_{free} for τ_{eff}.

For τ_{veg}, the use of s for the length-scale, L, in Eq. (S4b) inherently assumes the conditions $s < d$, where d is the cylinder diameter, which is equal to b_v for the seagrasses/marshes, where otherwise d should be applied for L (Tanino and Nepf, 2008; Nepf, 2012). In our analysis performed in the main text, the cylinder approximations (Fig. 3) did not satisfy the conditions $s < d$, thus the d (= b_v) would be appropriate for L.

Based on these, we modified Eqs. (S3–4) as

$$D_w = c_2 \frac{P_w}{\tau_{veg}} \quad \text{(S5)}$$

$$\tau_{veg} = \left(\frac{L^2}{{c_w}^2 P_w}\right)^{1/3} = \left(\frac{{b_v}^2}{{c_w}^2 P_w}\right)^{1/3} \quad \text{(S6)}$$

These modified equations were used for the model analysis using the cylinder array approximations in the main text.

Text S3. *Rhizophora* root model

The vertical profile of root projected area density (a_{root}) was computed using the empirical model for *Rhizophora* root structures (*Rh*-root model) proposed by Yoshikai et al. (2021); the procedure is summarized below.

The model was designed to predict the structure of the individual root system. It predicts the vertical profile of the number of roots of a tree using two parameters–*S* (scaling factor) and HR_{max} (maximum root height). The *S* and HR_{max} are strongly related to tree size represented by the stem diameter measured at 1.3-m height (D_{stem}). The k^{th} highest root in a root system can be then expressed as

$$HR_k = HR_{max} S^{(k-1)} \geq HR_{min} \quad \text{(S7a)}$$

$$S = 1 - \beta_S {D_{stem,i}}^{\alpha_S} \quad \text{(S7b)}$$

$$HR_{max} = \alpha_{HR} D_{stem,i} + \beta_{HR} \quad \text{(S7c)}$$

where HR_{min} in Eq. (S7a) is a model parameter (critical root height) that limits the minimum root height of a tree, $D_{stem,i}$ is the stem diameter (m) where the subscript "*i*" represents tree index, and α_S, β_S, α_{HR}, β_{HR} are the scaling parameters for *S* and HR_{max}, respectively. The α_S, β_S, α_{HR}, β_{HR} are considered site- and species-specific parameters, thus the values need to be derived through a field survey. See Yoshikai et al. (2021) or (2022a) for the procedure to obtain these parameter values in the field with reduced workload. The value of HR_{min} also needs to be determined for a site through a field survey.

From Eq. (S7), the heights of all roots of a tree can be predicted. Yoshikai et al. (2022a) suggested that the individual roots can be approximated as a linear shape to estimate the projected area of roots. The linear shape of a root projected from the direction along the *x*-axis can be expressed as

$$z = (tan\theta_l)\left(\frac{y}{cos\psi}\right) + HR \qquad \text{where } 0 < z < HR \quad \text{(S8)}$$

where *y* and *z* represent the horizontal and vertical coordinate of a point, where $y = 0$ at the location where a root emerges from the stem or another root and $z = 0$ at the ground, *HR* is the height of a root (m), θ_l is the angle of the approximated linear shape relative to the horizontal axis, and ψ is the azimuth root angle around the *z*-axis relative to the *x*-axis. The

value of θ_l was empirically determined in Yoshikai et al. (2022a). The projected area of a root can be calculated by multiplying the root length provided by Eq. (S8) and the mean root diameter ($D_{root,ave}$). Then, by summing up the projected areas of all the roots per vertical height interval, dz (0.05 m in this study), the vertical profile of root projected area per dz of a tree "i" ($A_{root,i}(z)$ (m^2)) can be calculated. Here, because the root azimuth angle in Eq. (8), ψ, is unknown, Yoshikai et al. (2022a) employed random numbers to ψ and estimated $A_{root,i}$ from the ensemble approach. Based on the ensemble computations, we found that the $A_{root,i}$ computed using random numbers for ψ is approximately 80 % of the $A_{root,i}$ computed using the zero value for ψ for all the roots, which is referred to as $A_{root0,i}$ below. Hence, we calculated the $A_{root,i}$ as

$$A_{root,i}(z) = 0.8 \times A_{root0,i}(z) \quad \text{(S9)}$$

where the multiplication by 0.8 represents the effects of random azimuth angle on the projected area. This approach (Eq. S9) does not require the ensemble approach to estimate $A_{root,i}$, which is convenient for implementation to the numerical model.

Text S4. Tree census data

We used tree census data collected from three sites–two from Bakhawan Ecopark, Aklan, Philippines (11° 43' N, 122° 23' E; Suwa et al., unpublished data), and one from Fukido River mangrove forest, Ishigaki, Japan (24° 20' N, 124° 15' E; Suwa et al., 2021)–to investigate the validity of the proposed parameterization of tree size variations (see Section 2.1.3). We refer to the two sites of Bakhawan Ecopark as Bak1 and Bak2, respectively, and Fukido River mangrove forest as Fuk.

The sites Bak1 and Bak2 are 30-year-old and 17-year-old planted stands, respectively, of *Rhizophora apiculata*; Bak2 includes the site where the vegetation and hydrodynamic data were collected by Yoshikai et al. (2022a), which were used for model evaluation in this study. The site Fuk is a natural mangrove forest vegetated by *Rhizophora stylosa* and *Buruguiera gymnorrhiza*. Along with the soil salinity gradient, a notable change in the forest structural variables (stem diameter, tree height, species composition) was observed at this forest (Yoshikai et al., 2022b). As described in Suwa et al. (2021), a 7-m radius circular plot was established and the stem diameter at 1.3-m height (D_{stem}) was measured for all the trees. The number of plots for the tree census is 6 for Bak1, 6 for Bak2, and 14 for Fuk, respectively. We did not use the data of 10 plots out of a total of 24 plots in Fuk collected in Suwa et al. (2021) because of the absence of *R. stylosa* trees.

The root structures of *R. apiculata* and *R. stylosa* at these three sites were investigated in Yoshikai et al. (2021) and the values of the *Rh*-root model parameters were derived (Table S1). These parameter values were used for the computation of the vertical profile of root projected area per *dz* of a tree, $A_{root,i}(z)$, for each site using the *Rh*-root model; these are shown in Fig. 2.

Table S1. *Rhizophora* root model parameters for three tree census sites.

Parameter	Bak1	Bak2	Fuk
Scaling parameter for S (α_S)	–0.91	–2.04	–1.76
Scaling parameter for S (β_S)	$10^{-2.00}$	$10^{-3.59}$	$10^{-3.18}$
Scaling parameter for S (α_{HR})	2.06	15.38	2.71
Scaling parameter for S (β_{HR})	0.82	0.08	0.50
Critical root height (HR_{min}, m)	0.01[a]	0.01	0.01[a]
Root angle of approximated linear root shape (θ_l, degree)	–34.5[a]	–34.5	–41.9
Mean root diameter ($D_{root,ave}$, m)	0.03[a]	0.03	0.03

[a] Value determined for Bak2 was used.

Table S2. Sediment parameter settings for the sediment transport simulation using the COAWST. The effect of critical shear stress for deposition was damped out by giving very high values.

Parameter	Value	References
Suspended sediment concentration at the upstream boundary (mg L^{-1})	50	e.g., Mariotti and Fagherazzi (2010), Horstman et al. (2015), Xie et al. (2020)
Sediment grain density (kg m^{-3})	2650	e.g., Xie et al. (2020)
Porosity	0.7[a]	
Sediment layer thickness (m)	1.0[a]	
Settling velocity (mm s^{-1})	0.1	Horstman et al. (2015), D'Alpaos and Marani (2016), Willemsen et al. (2016)
Erosion rate (kg m^{-2} s^{-1})	3×10^{-4}	e.g., Mariotti and Fagherazzi (2010), D'Alpaos and Marani (2016)

Critical shear stress for erosion (τ_{cr}, N m^{-2})	0.1	Horstman et al. (2015)
Critical shear stress for deposition (N m^{-2})	1000[a]	

[a] Assumed.

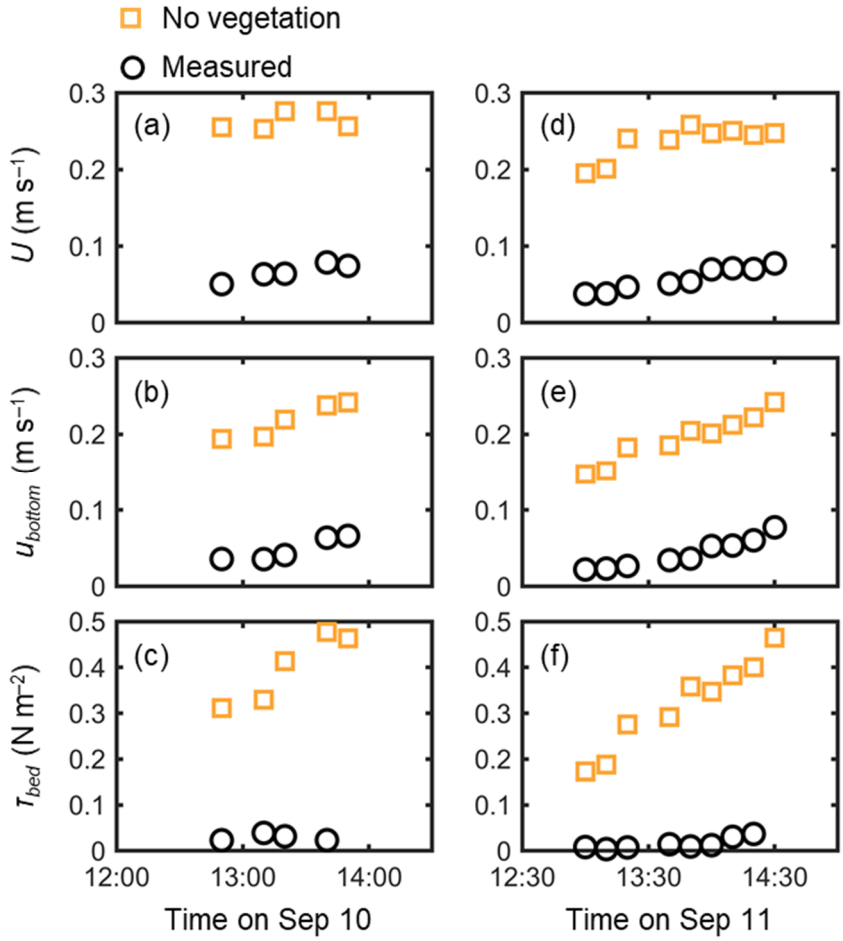

Figure S1. Time-series of measured and predicted (a, d) cross-sectional mean velocity (U), (b, e) (spatially averaged) velocity at z = 0.05 m, and (c, f) bed shear stress (τ_{bed}) during the two-days measurement in Bakhawan Ecopark. The measured values are from Yoshikai et al. (2022a) and the predicted values are obtained through the COAWST without imposing vegetation drag (no vegetation).

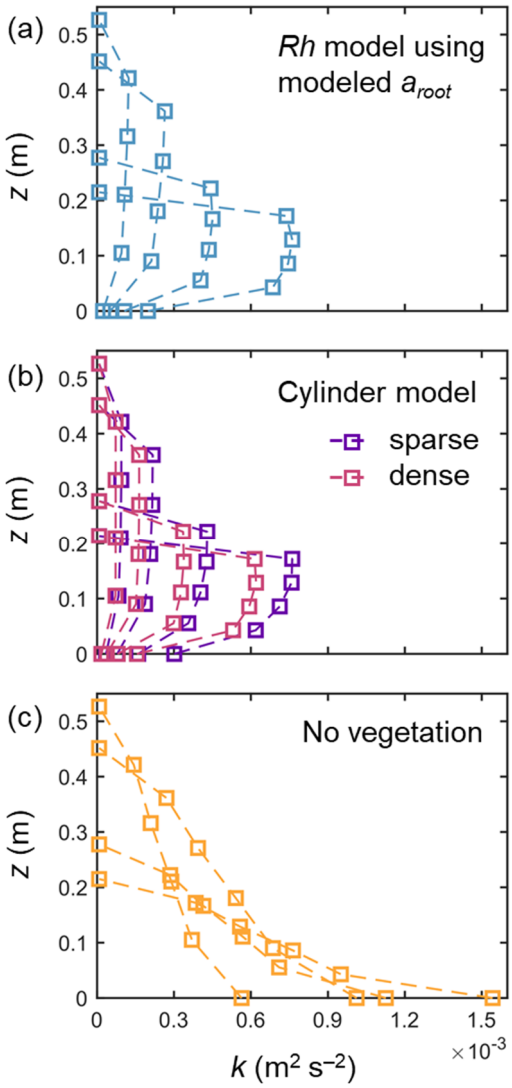

Figure S2. Vertical profiles of turbulent kinetic energy (k) predicted by the COAWST employing (a) *Rh* model using modeled root projected area density profile (a_{root}), (b) cylinder model with sparse and dense arrays, and (c) without imposing vegetation drag (no vegetation) for some tidal phases corresponding to the ones shown in Fig. 5.

References

Baptist, M. J., Babovic, V., Rodríguez Uthurburu, J., Keijzer, M., Uittenbogaard, R. E., Mynett, A., & Verwey, A. (2007). On inducing equations for vegetation resistance. Journal of Hydraulic Research, 45(4), 435–450. https://doi.org/10.1080/00221686.2007.9521778.

Beudin, A., Kalra, T. S., Ganju, N. K., & Warner, J. C. (2017). Development of a coupled wave-flow-vegetation interaction model. Computers & Geosciences, 100, 76–86. https://doi.org/10.1016/j.cageo.2016.12.010.

D'Alpaos, A., & Marani, M. (2016). Reading the signatures of biologic–geomorphic feedbacks in salt-marsh landscapes. Advances in water resources, 93, 265–275. https://doi.org/10.1016/j.advwatres.2015.09.004.

Defina, A., & Bixio, A. C. (2005). Mean flow and turbulence in vegetated open channel flow. Water Resources Research, 41(7). https://doi.org/10.1029/2004WR003475.

Horstman, E. M., Dohmen-Janssen, C. M., Bouma, T. J., & Hulscher, S. J. (2015). Tidal-scale flow routing and sedimentation in mangrove forests: Combining field data and numerical modelling. Geomorphology, 228, 244–262. https://doi.org/10.1016/j.geomorph.2014.08.011.

King, A. T., Tinoco, R. O., & Cowen, E. A. (2012). A *k–ε* turbulence model based on the scales of vertical shear and stem wakes valid for emergent and submerged vegetated flows. Journal of Fluid Mechanics, 701, 1–39. https://doi.org/10.1017/jfm.2012.113.

Liu, Z., Chen, Y., Wu, Y., Wang, W., & Li, L. (2017). Simulation of exchange flow between open water and floating vegetation using a modified RNG *k-ε* turbulence model. Environ Fluid Mech 17, 355–372. https://doi.org/10.1007/s10652-016-9489-5.

López, F., & García, M. H. (2001). Mean flow and turbulence structure of open-channel flow through non-emergent vegetation. Journal of Hydraulic Engineering, 127(5), 392–402. https://doi.org/10.1061/(ASCE)0733-9429(2001)127:5(392).

Mariotti, G., & Fagherazzi, S. (2010). A numerical model for the coupled long−term evolution of salt marshes and tidal flats. Journal of Geophysical Research: Earth Surface, 115(F1). https://doi.org/10.1029/2009JF001326.

Nepf, H. M. (2012). Flow and transport in regions with aquatic vegetation. Annual review of fluid mechanics, 44, 123–142. https://doi.org/10.1146/annurev-fluid-120710-101048.

Suwa, R., Rollon, R., Sharma, S., Yoshikai, M., Albano, G. M. G., Ono, K., ... & Nadaoka, K. (2021). Mangrove biomass estimation using canopy height and wood density in the South East and East Asian regions. Estuarine, Coastal and Shelf Science, 248, 106937. https://doi.org/10.1016/j.ecss.2020.106937.

Tanino, Y., & Nepf, H. M. (2008). Lateral dispersion in random cylinder arrays at high Reynolds number. Journal of Fluid Mechanics, 600, 339–371. https://doi.org/10.1017/S0022112008000505.

Willemsen, P. W. J. M., Horstman, E. M., Borsje, B. W., Friess, D. A., & Dohmen-Janssen, C. M. (2016). Sensitivity of the sediment trapping capacity of an estuarine mangrove forest. Geomorphology, 273, 189–201. https://doi.org/10.1016/j.geomorph.2016.07.038.

Xie, D., Schwarz, C., Brückner, M. Z., Kleinhans, M. G., Urrego, D. H., Zhou, Z., & Van Maanen, B. (2020). Mangrove diversity loss under sea-level rise triggered by bio-morphodynamic feedbacks and anthropogenic pressures. Environmental Research Letters, 15(11), 114033. https://doi.org/10.1088/1748-9326/abc122.

Yoshikai, M., Nakamura, T., Suwa, R., Argamosa, R., Okamoto, T., Rollon, R., ... & Nadaoka, K. (2021). Scaling relations and substrate conditions controlling the complexity of *Rhizophora* prop root system. Estuarine, Coastal and Shelf Science, 248, 107014. https://doi.org/10.1016/j.ecss.2020.107014.

Yoshikai, M., Nakamura, T., Bautista, D. M., Herrera, E. C., Baloloy, A., Suwa, R., Basina, R., Primavera-Tirol, Y. H., Blanco, A.C., & Nadaoka, K. (2022a) Field measurement and prediction of drag in a planted *Rhizophora* mangrove forest. Journal of Geophysical Research: Oceans, 127, e2021JC018320. https://doi.org/10.1029/2021JC018320.

Yoshikai, M., Nakamura, T., Suwa, R., Sharma, S., Rollon, R., Yasuoka, J., Egawa, R., & Nadaoka, K. (2022b). Predicting mangrove forest dynamics across a soil salinity gradient using an individual-based vegetation model linked with plant hydraulics. Biogeosciences, 19, 1813–1832. https://doi.org/10.5194/bg-19-1813-2022.